nature cell biology

# Regulation of mitotic entry by microcephalin and its overlap with ATR signalling

Gemma K. Alderton[1], Laura Galbiati[1], Elen Griffith[4], Katharina H. Surinya[2], Heidemarie Neitzel[3], Andrew P. Jackson[2,4], Penny A. Jeggo[1,5] and Mark O'Driscoll[1,5]

**Ataxia-telangiectasia mutated and Rad3 related (ATR)–Seckel syndrome and autosomal recessive primary microcephaly (MCPH) syndrome share clinical features. RNA interference (RNAi) of *MCPH1* have implicated the protein it encodes as a DNA-damage response protein that regulates the transcription of *Chk1* and *BRCA1*, two genes involved in the response to DNA damage[1,2]. Here, we report that truncating mutations observed in MCPH-syndrome patients do not impact on *Chk1* or *BRCA1* expression or early ATR-dependent damage-induced phosphorylation events. However, like ATR–Seckel syndrome cells, *MCPH1*-mutant cell lines show defective G2–M checkpoint arrest and nuclear fragmentation after DNA damage, and contain supernumerary mitotic centrosomes. *MCPH1*-mutant and ATR–Seckel cells also show impaired degradation of Cdc25A and fail to inhibit Cdc45 loading onto chromatin after replication arrest. Additionally, microcephalin interacts with Chk1. We conclude that MCPH1 has a function downstream of Chk1 in the ATR-signalling pathway. In contrast with ATR–Seckel syndrome cells, *MCPH1*-mutant cells have low levels of Tyr 15-phosphorylated Cdk1 (pY15-Cdk1) in S and G2 phases, which correlates with an elevated frequency of G2-like cells displaying premature chromosome condensation (PCC)[3,4]. Thus, MCPH1 also has an ATR-independent role in maintaining inhibitory Cdk1 phosphorylation, which prevents premature entry into mitosis.**

Primary microcephaly (OMIM 251200) is a recessive disorder that is characterised by a markedly reduced brain size. The first causative gene identified encodes MCPH1, (microcephalin; also known as BRIT1), a protein with three Brca1 carboxy-terminal (BRCT) domains[3,4]. Seckel syndrome, another microcephalic syndrome, can be caused by hypomorphic mutations in *ATR* or defective ATR signalling[5,6]. ATR and ataxia-telangiectasia mutated (ATM) are protein kinases that regulate overlapping damage-response pathways. ATM responds to DNA double-strand breaks (DSBs), whereas ATR is activated by single stranded DNA, which arises during replication-fork stalling and certain DNA repair processes[7,8]. ATR, but not ATM, is essential for cell survival. Phosphorylation of the histone variant H2AX, an early step in both pathways, mediates assembly of a multiprotein complex (including p53 binding protein 1 (53BP1), mediator of DNA damage checkpoint protein 1 (MDC1) and BRCA1) at the damage site[9]. Chk1 and Chk2 function as transducer kinases. Activation of the damage response causes checkpoint arrest, stabilisation of stalled replication forks, and inhibition of replicon initiation and late origin firing. ATR–Seckel syndrome cells show reduced phosphorylation of H2AX and Chk1 after replication stalling, reduced stabilisation of stalled replication forks and a failure to effect G2–M arrest[5,6,10].

Here, we evaluate MCPH1 function in the DNA damage response using cell lines derived from MCPH syndrome patients. As the clinical features of MCPH syndrome patients resemble ATR–Seckel syndrome patients (see Supplementary Information) and not ATM-defective ataxia telangiectasia patients, we focused on the analysis of ATR-dependent signalling following replication fork arrest.

Lymphoblastoid cell lines (LBLs) with different truncating mutations in *MCPH1* ($MCPH1^{C74G}$ and $MCPH1^{427insA}$) were analysed. $MCPH1^{C74G}$ cells show reduced but residual MCPH1 protein expression, whereas $MCPH1^{427insA}$ cells lack detectable MCPH1 (Fig. 1a). The $MCPH1^{427insA}$, but not the $MCPH1^{C74G}$, transcript undergoes nonsense mediated decay (NMD); however, residual $MCPH1^{427insA}$ mRNA is detectable (see Supplementary Information, Fig. S1c). These cell lines were compared with an ATR–Seckel cell line, an ATM-defective cell line and a control LBL for their ability to effect ATR-dependent damage responses. Examination of the phosphorylation of H2AX, Chk1, Nbs1 and p53 after replication fork stalling revealed that whereas ATR–Seckel cells showed impaired phosphorylation, the ATM-defective cell line and the *MCPH1*-mutant lines showed a normal response (Fig. 1b–e). Although previous studies using *MCPH1* siRNA reported reduced Chk1 and BRCA1 protein levels[1,2], normal levels of Chk1, BRCA1 and phosphorylated Chk1 were observed in *MCPH1*-mutant cells (Fig. 1d and see Supplementary Information, Fig. S1a). 53BP1 foci formation

[1]Genome Damage and Stability Centre, University of Sussex, East Sussex, BN1 9RQ, UK. [2]Molecular Medicine Unit, University of Leeds, UK. [3]Institute of Human Genetics, Charite´Universitary Medicine, Berlin, Germany. [4]MRC Human Genetics Unit, Western General Hospital, Crewe Road, Edinburgh, EH4 2XU, UK. [5]Correspondence should be addressed to P.A.J. or M.O'D. (e-mail: p.a.jeggo@sussex.ac.uk; M.O-Driscoll@sussex.ac.uk)

Received 8 February 2006; accepted 30 May 2006; published online 18 June 2006; DOI: 10.1038/ncb1431

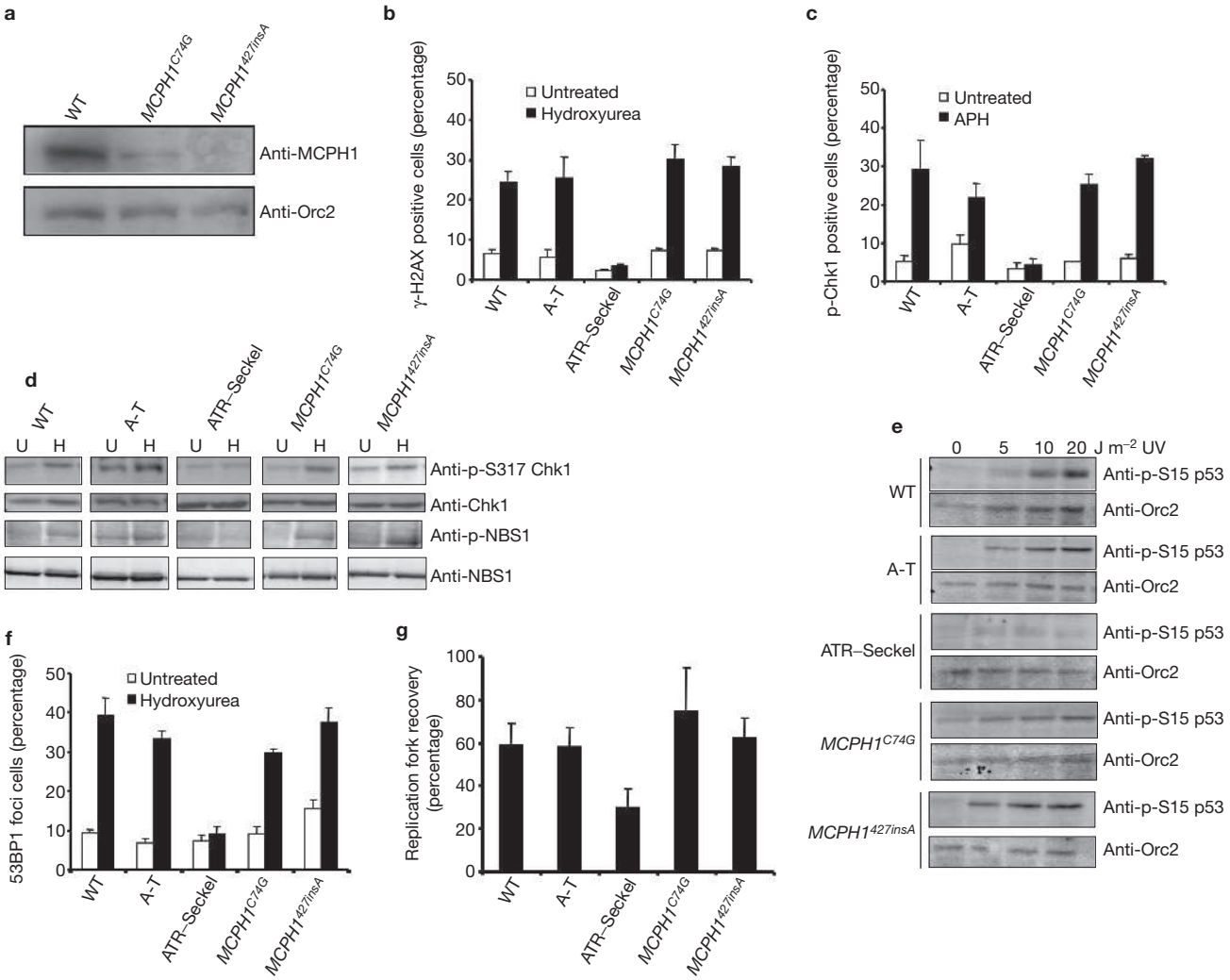


**Figure 1** *MCPH1*-mutant cell lines are proficient in upstream activation of ATR-dependent damage signalling. Lymphoblastoid cell lines (LBLs) from control (WT), an ATM-defective ataxia telangiectasia (A-T), an ATR-Seckel and two MCPH syndrome (*MCPH1*$^{C74G}$ and *MCPH1*$^{427insA}$) patients were examined for activation of ATR-dependent damage responses following replication fork arrest. (**a**) Western blot of extracts from the indicated cells using anti-MCPH1 with Orc2 as a loading control. (**b**) Induction of γ-H2AX after treatment with hydroxyurea. Cells were treated with 5 mM hydroxyurea for 1 h and the percentage of cells positive for γ-H2AX was scored using immunofluorescence microscopy. (**c**) Phosphorylation of Chk1 after treatment with APH. Cells were treated with 0.1 μM APH for 2 h and the percentage of cells positive for p-Chk1 (using an anti-pS317 Chk1 antibody) was scored using immunofluorescence microscopy. (**d**) Whole cell extracts (50 μg) from cells treated with 50 μM hydroxyurea were examined by western blotting using anti-p-S317 Chk1 or anti-p-Nbs1 antibodies. Loading was assessed using anti-Chk1 or anti-Nbs1 antibodies. U, untreated; H, hydroxyurea. (**e**) p53 phosphorylation after UV treatment. Cells were treated with the indicated dose of UV, incubated for 2 h and examined by western blotting using anti-pS15 p53 antibodies 2 h after treatment. Orc2 was used as a loading control. (**f**) 53BP1 foci formation after hydroxyurea treatment. Cells were treated as in **b** and the percentage of cells with more than five 53BP1 foci were scored using immunofluorescence microscopy. (**g**) Stabilization of stalled replication forks. Replication forks were marked by pulse labelling with CldU, arrested by treating with APH (10 μM) for 2 h and fork progression monitored following removal of APH in the presence of IdU. The error bars represent the s.d. of at least three independent experiments.

after hydroxyurea treatment, which is Chk1 and ATR dependent[10–12], occurred normally in the *MCPH1*-mutant cell lines but was reduced in ATR–Seckel cells (Fig. 1f). Addition of the Chk1 inhibitor SB-218078 abolished 53BP1 foci formation, thus verifying the requirement for Chk1 (see Supplementary Information, Fig. S2b). Recovery of DNA synthesis after replication arrest is also Chk1 and ATR-dependent. To monitor this process, DNA replication was visualised using fluorescently labelled antibodies specific for halogenated deoxyuridine (dU) derivatives[10,13]. Control and *MCPH1*-mutant cells showed replication recovery in contrast with ATR–Seckel cells (Fig. 1g). SB-218078 diminished replication fork recovery (see Supplementary Information, Fig. S2a). Collectively, these data show that *MCPH1*-mutant cells activate ATR signalling, Chk1 is phosphorylated normally and at least two upstream steps of the ATR–Chk1-dependent damage response are regulated. These findings suggest that the cellular and clinical features of MCPH syndrome patient cells cannot be attributed to MCPH1-dependent transcriptional regulation of *Chk1* or *BRCA1*. ATR-dependent G2–M arrest in *MCPH1*-mutant cells was assessed using the cytokinesis block proliferation index (CBPI) assay[10,14]. Following DNA damage, cytochalasin B was added to block cytokinesis. Less than 50% of untreated cells were mononucleate, demonstrating progression through mitosis during the 72 h incubation. Following treatment of control and ATM-defective cells with aphidicolin (APH), hydroxyurea or UV radiation, the percentage of mononucleate cells increases approximately twofold, indicative of G2–M checkpoint

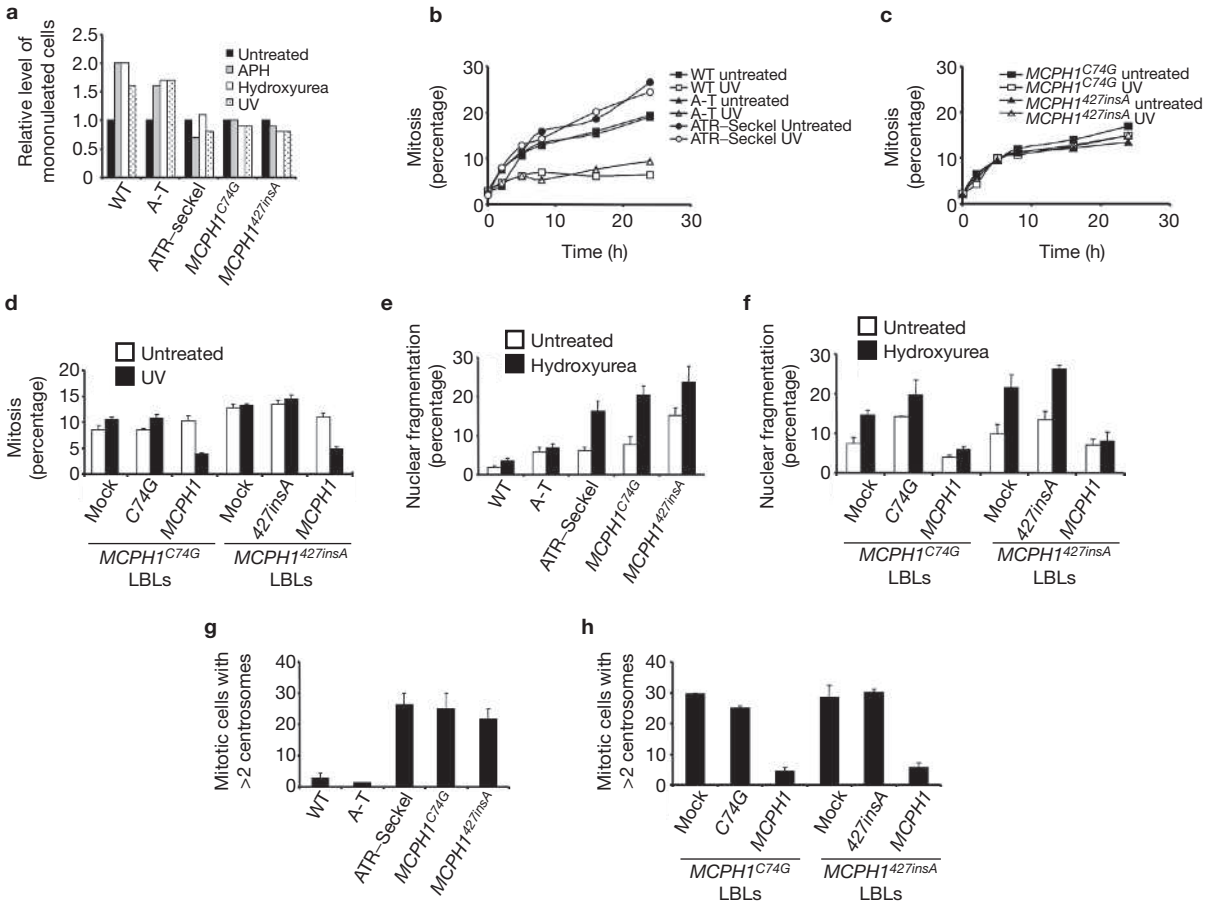


**Figure 2** *MCPH1*-mutant cell lines show defects in downstream ATR-dependent phenotypes. (**a**) *MCPH1*-mutant cells show defective G2–M checkpoint arrest using the CBPI assay. Cells were treated with APH (0.1 μM for 2 h), hydroxyurea (0.2 mM for 2 h) or UV (2.5 J m$^{-2}$) and the level of mononucleate/mono + bi-nucleate cells examined after 72 h incubation in cytochalasin B (5 μg ml$^{-1}$). Results are expressed relative to untreated cells. (**b**, **c**) G2/M checkpoint arrest is observed 5 h post UV treatment in control but not *MCPH1*-mutant or ATR-Seckel cells. The mitotic index was examined at varying times following treatment with 2.5 J m$^{-2}$ UV in the presence of nocodazole. (**d**) Defective UV-induced G2–M arrest is complemented by transfection of *MCPH1*-mutant cells with wild-type (WT) but not mutant *MCPH1*cDNA. *MCPH1$^{C74G}$* cDNA (*C74G*) was introduced into the *MCPH1$^{C74G}$* cell line and *MCPH1$^{427insA}$* cDNA (*427insA*) was introduced into the *MCPH1$^{427insA}$* cell line. Mock and *MCPH1* represent transfection with empty vector or wild-type *MCPH* cDNA, respectively. (**e**) Nuclear fragmentation was examined 24 h after treatment with 5 mM hydroxyurea. The percentage of cells displaying nuclear fragmentation is shown. (**f**) Wild-type but not mutant *MCPH1*cDNA corrects the nuclear fragmentation phenotype. Nuclear fragmentaion was examined 24 h after treatment with 5 mM hydroxyurea, which commenced 24 h after transfection. (**g**) MCPH1 cells show elevated levels of mitotic cells with supernumerary centrosomes. The percentage of mitotic (phospho-S10-histone H3 positive cells) with > 2 centrosomes was determined following 24 h incubation with nocodozole. (**h**) Wild-type but not mutant *MCPH1*cDNA reduces the percentage of cells with supernumery centrosomes. *MCPH1*-mutant cells were doubly transfected with wild-type or mutant *MCPH1*cDNA and examined 48 h after the second transfection. The error bars represent the s.d. of at least three independent experiments.

arrest (Fig. 2a). This increase is not observed in ATR–Seckel or *MCPH1*-mutant cell lines, indicating defective G2–M arrest (Fig. 2a).

The time course of G2–M arrest was also examined by analysing the mitotic index in nocodazole-arrested cells that were either untreated or incubated for varying times after UV irradiation (2.5 J m$^{-2}$). Control and ATM-defective cells showed a significant decrease in the mitotic index observed at 5 h and this was maintained up to 24 h after UV treatment, unlike the ATR–Seckel and *MCPH1*-mutant cell lines (Fig. 2b, c). This defect was corrected in both *MCPH1*-mutant cell lines following transfection with full length *MCPH1* cDNA, but not when mutant *MCPH1* cDNA was introduced into the respective *MCPH1*-mutant cell line (Fig. 2d). Thus, MCPH1 has a function downstream of Chk1 that affects the ATR-dependent G2–M checkpoint.

Replication fork arrest induces nuclear fragmentation in ATR–Seckel cells[6]. Following treatment of ATR–Seckel and *MCPH1*-mutant cells with hydroxyurea (5 mM), there was a significant increase in cells displaying nuclear fragmentation, but not in hydroxyurea-treated control or ATM-defective cells (Fig. 2e). Although the *MCPH1$^{427insA}$* cell line showed a high endogenous level of nuclear fragmentation, this increased after treatment with hydroxyurea. The nuclear fragmentation phenotype was corrected following introduction of wild-type *MCPH1* cDNA into *MCPH1*-mutant cells. Neither mutant *MCPH1* cDNA corrected the respective *MCPH1*-mutant cell line (Fig. 2f).

Another phenotype observed in ATR–Seckel cells is the presence of endogenous supernumerary mitotic centrosomes[6]. Strikingly, both *MCPH1*-mutant cell lines, but not control or ATM-defective cells, exhibit elevated frequencies of mitotic cells with supernumerary centrosomes (approximately 25%; Fig. 2g). Furthermore, this phenotype was corrected with wild-type but not mutant *MCPH1* cDNA (Fig. 2h). Transfection with *ATR* cDNA complemented these defects in ATR–Seckel cells[6].

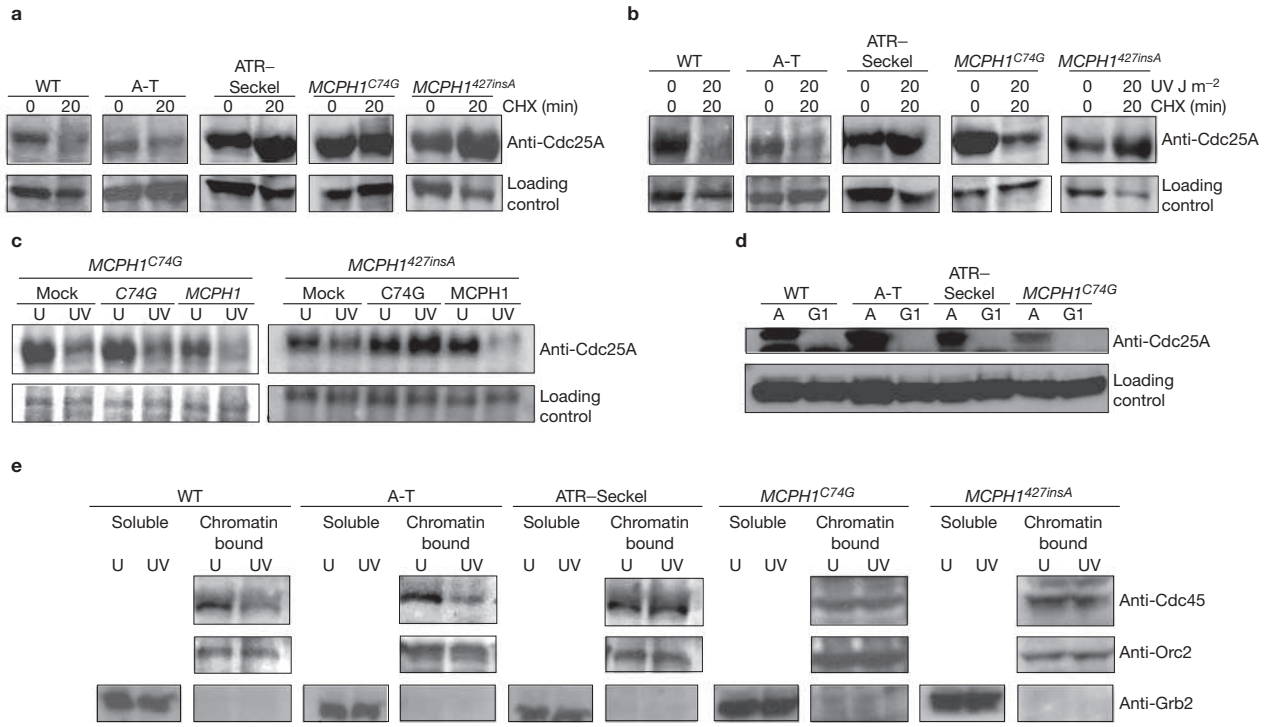


**Figure 3** ATR–Seckel and *MCPH1*-mutant cells show impaired Chk1-dependent degradation of Cdc25A. (**a**) Unirradiated cells were treated with cycloheximide (CHX; 100 μg ml$^{-1}$) for 20 mins before extraction and western blotting using anti-Cdc25A antibodies. Loading was controlled using a non-specific band consistently obtained with anti-Cdc25A antibodies. (**b**) Degradation of Cdc25A following UV irradiation. Untreated cells untreated or cells UV-irradiated in the presence of cyclohexamide and maintained in cyloheximide for 20 min after irradiation, were processed for western blotting using anti-Cdc25A antibodies. (**c**) *MCPH1*-mutant cells regain the ability to degrade Cdc25A after UV (20 J m$^{-2}$) and cyloheximide treatment after transfection with wild-type but not mutant *MCPH1*cDNAs. U, untreated; UV, UV irradiated. (**d**) ATR and *MCPH1*-mutant cells are proficient in the degradation of Cdc25A in G1 phase. Primary fibroblasts were serum starved and the levels of Cdc25A examined by western blotting. A, asynchronous; G1, serum starved. (**e**) Cdc45 chromatin loading is impaired in ATR–Seckel and *MCPH1*-mutant cells after UV treatment. Cells were untreated (U) or treated with UV (20 J m$^{-2}$) and fractionated to obtain chromatin bound versus soluble proteins. The proteins were analysed by western blotting using anti-Cdc45 antibodies. Grb2 was used to verify the absence of soluble proteins in the chromatin bound fraction. Orc2 represents the loading control for chromatin bound protein.

The Cdc25A phosphatase, which regulates mitotic entry, is phosphorylated by Chk1, thus targeting it for ubiquitin-dependent degradation[15–19]. This occurs during unperturbed cell growth and is amplified following DNA damage[20]. The stability of Cdc25A was examined in undamaged cells after 20 mins incubation in cycloheximide. Although the level of Cdc25A decreased dramatically in control and ATM-defective cells, as previously reported[20], ATR–Seckel and *MCPH1*-mutant cells showed diminished Cdc25A degradation (Fig. 3a). Even after UV treatment, which elevates Cdc25A degradation in control cells, Cdc25A levels remained stable in ATR–Seckel and *MCPH1*$^{427insA}$ cells (Fig. 3b). Some degradation was observed in *MCPH1*$^{C74G}$ cells, possibly indicating leakiness, but detectable Cdc25A levels remained in contrast with control and ATM-defective cells. Introduction of wild-type, but not mutant, *MCPH1* cDNAs into the respective *MCPH1*-mutant cells restored UV-induced Cdc25A turnover (Fig. 3c).

Following mitotic exit, Cdc25A is degraded in an APC/C$^{Cdh1}$ dependent manner[21]. Cdc25A levels were examined in G1-arrested plateau-phase primary fibroblasts. Control, ATM-defective, ATR–Seckel and *MCPH1*-mutant (derived from the *MCPH1*$^{C74G}$ patient) fibroblasts all exhibited undetectable levels of Cdc25A under these conditions (Fig. 3d), suggesting that APC/C$^{Cdh1}$-dependent degradation of Cdc25A occurs normally in ATR–Seckel and *MCPH1*-mutant cells. These findings demonstrate that MCPH1 and ATR are required for Cdc25A degradation during unperturbed cell growth and after DNA damage, but are dispensable for APC/C$^{Cdh1}$-dependent degradation on exit from mitosis.

Cdc25A regulates Cdk2–cyclin A/E in S phase, which influences Cdc45 chromatin loading following DNA damage[22]. Cdc45 has an essential role in the initiation of DNA replication[23,24]. The chromatin retention of Cdc45 was examined 1 h after treatment with 20 J m$^{-2}$ UV. Decreased levels of chromatin-bound Cdc45 were observed in control and ATM-defective cells, but not in ATR–Seckel or *MCPH1*-mutant cells, demonstrating that diminished Cdc25A degradation potentially effects the intra-S phase checkpoint arrest (Fig. 3e). ATM-defective cells show a normal response as ATM is not activated by UV radiation.

Cdc25 phosphatases also regulate Cdk1–cyclin B1 activity, and hence mitotic entry, by reversing inhibitory Y15–T14-Cdk1 phosphorylation[25]. To determine whether the failure of *MCPH1*-mutant and ATR–Seckel cells to degrade Cdc25A impacts on mitotic entry, cumulative mitotic indices were monitored following release from synchronisation at the G1–S boundary (Fig. 4a). All cell lines commenced mitotic entry 4–10 h after release from synchronisation. Strikingly, the two *MCPH1*-mutant cell lines reproducibly exhibited low pY15-Cdk1 levels that were evident from 2 h after release (Fig. 4c). pY15-Cdk1 levels were decreased in control, ATM-defective and ATR–Seckel cells at 4 h after release. The expected correlation of mitotic entry and reduced pY15-Cdk1 levels was not observed at later times after release, most likely due to incomplete synchronisation (Fig. 4c shows the 0, 2 and 4 h samples). However, the reduced pY15-Cdk1 levels in *MCPH1*-mutant cells were marked and reproducible. Although *MCPH1*-mutant and control cells showed a

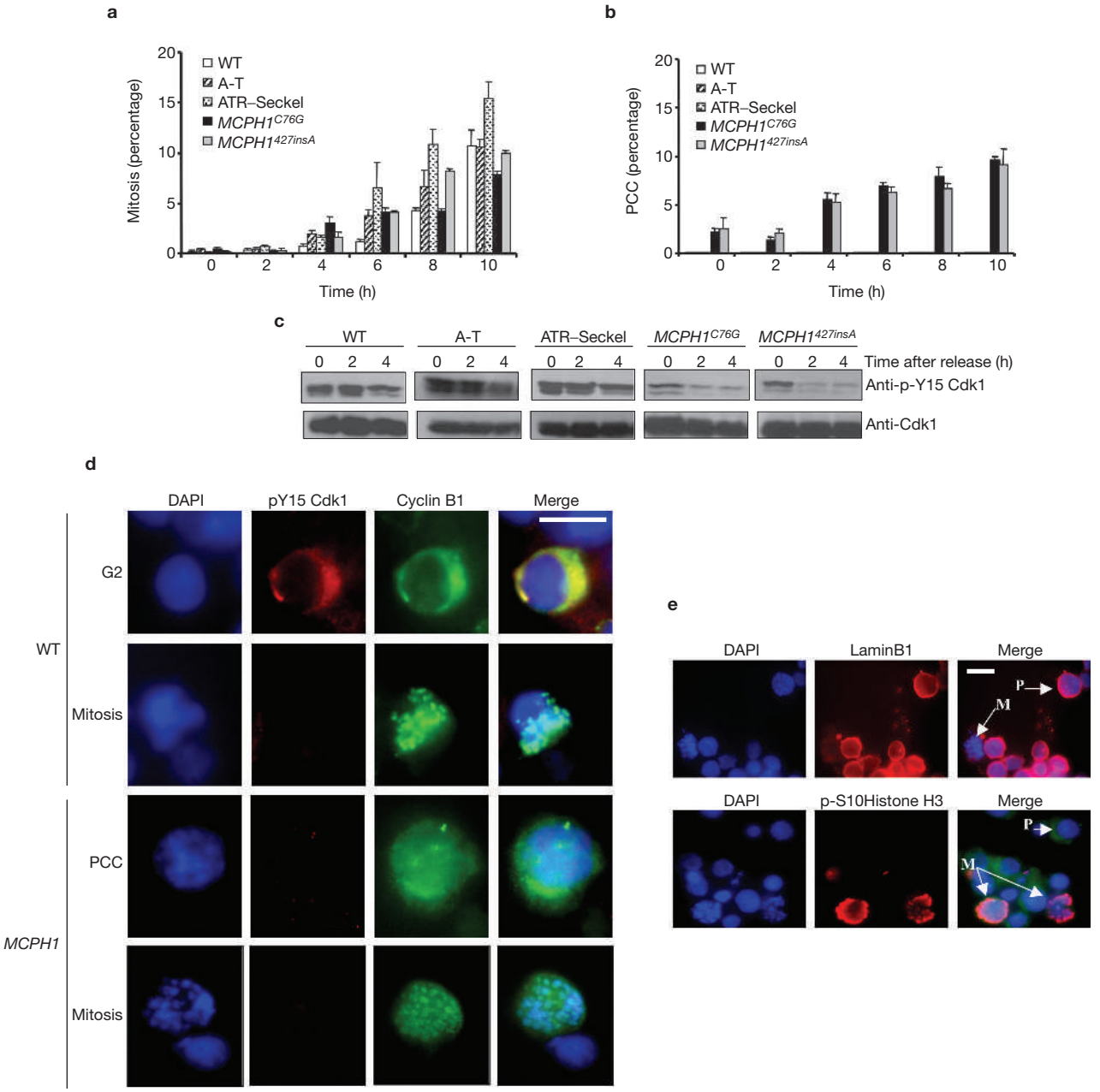


**Figure 4** *MCPH1*-mutant cells but not ATR–Seckel cells show rapid loss of p-Y15 Cdk1 following S phase progression that correlates with PCC formation. (**a**–**c**) Exponentially growing cells were synchronised overnight with 0.2 mM mimosine. Following release from synchronisation, cells were treated with nocodazole to prevent mitotic exit and were examined at 2 h intervals for mitotic index (**a**), PCC formation (**b**) and by western blotting using anti-pY15 Cdk1 or anti-Cdk1 antibodies (**c**). PCCs were not observed in control, A-T or ATR–Seckel cells (no vertical bars in the graph). The results shown for western blotting are the 0, 2 and 4 h samples but 6 and 8 hr samples gave similar results to the 4 h sample. (**d**) Immunofluorescence microscopy analysis shows *MCPH1*-mutant cells have decreased cytoplasmic colocalized pY15-Cdk1 and cyclin B1 staining. Cells were examined using anti-pY15 Cdk1 and anti-cyclin B1 antibodies. Mitotic cells were visible in all populations. Representative cells from wild-type and $MCPH1^{C74G}$ cells are shown. *MCPH1*-mutant PCC cells show dispersed cyclin B1 staining and low or undetectable pY15-Cdk1. (**e**) Immunofluorescence microscopy shows that PCC cells exhibit G2 rather than mitotic characteristics. *MCPH1*-mutant cells were examined by staining with the nuclear envelope protein, Lamin B1 or the mitotic marker pS10 histone H3 (bottom). Normal mitotic cells with pS10-histone H3 but no lamin B1 staining were observed (arrow, M). PCC cells (arrow, P) retained an intact nuclear envelope (evident by lamin B1 staining) and did not express pS10-histone H3. Representative $MCPH1^{C74G}$ cells are shown.The error bars represent the s.d. of at least three independent experiments. The scale bars represent 10 µm.

similar timing of mitotic entry, the decrease in pY15-Cdk1 precedes the increased appearance of cells with PCCs (Fig. 4b and see Supplementary Information for a detailed description of the PCC phenotype). PCC cells were not observed in control or ATR–Seckel cells (Fig. 4b and see Supplementary Information, Table s1). UV treatment had no significant impact on pY15-Cdk1 levels in any line or on PCC formation in the *MCPH1*-mutant cells (data not shown). The synchronised control and ATM-defective lines showed the expected UV-induced G2–M checkpoint arrest, which was abolished in the synchronised ATR–Seckel or *MCPH1*-mutant lines (data not shown).

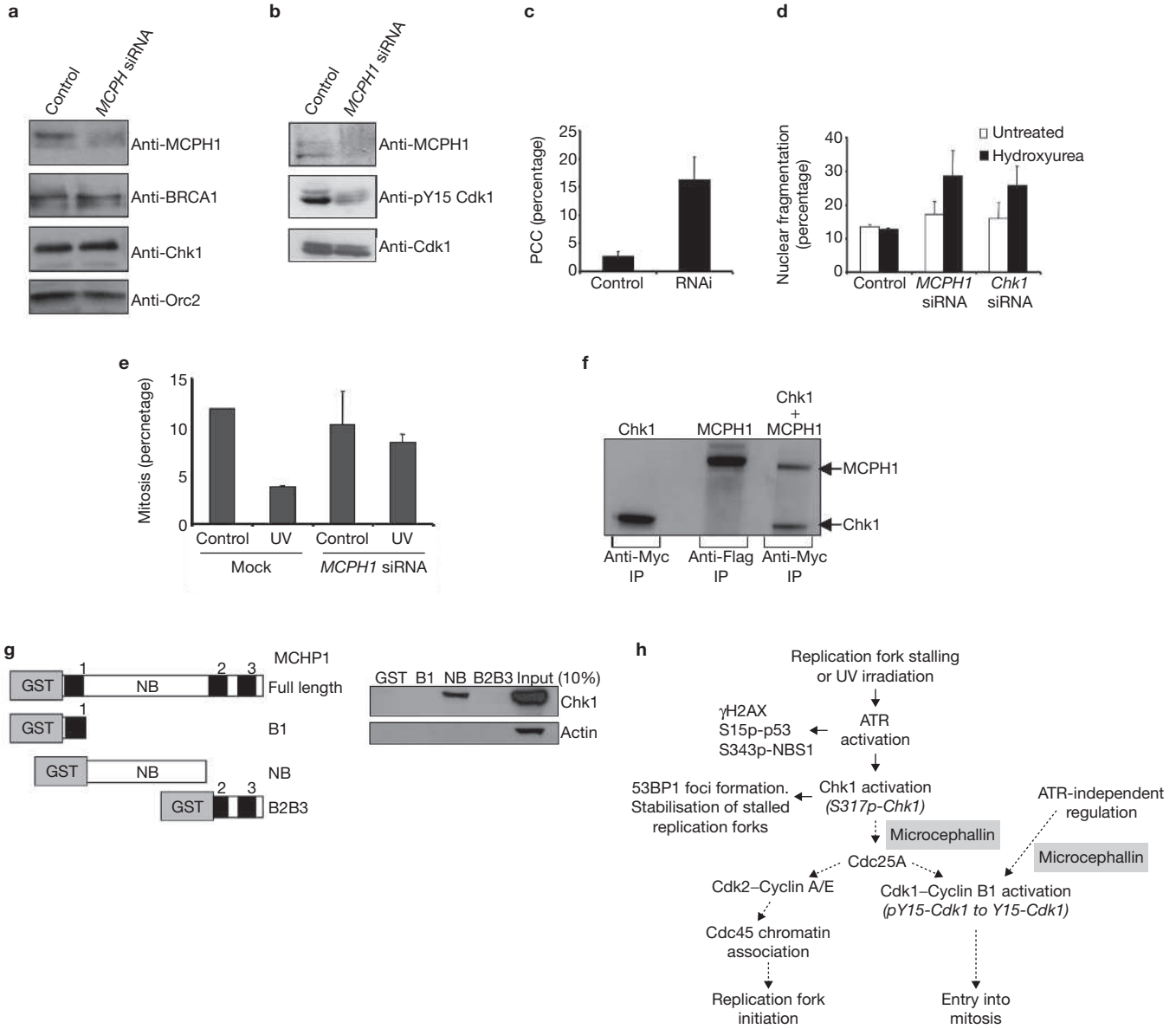


**Figure 5** *MCPH1* siRNA confers the phenotype observed in MCPH1 patient cells. (**a**, **b**) Control LBLs were treated with siRNA oligonucleotides directed to GFP (control) or *MCPH1*. *MCPH1* siRNA (**a**) caused decreased *MCPH1* but not *Chk1* or *BRCA1* expression and decreased pY15 Cdk1 levels (**b**) in unsynchronised cells. (**c**) PCC formation. *MCPH1* siRNA caused a small increase in PCCs. **(d)** Control siRNA caused some nuclear fragmentation which increased after hydroxyurea treatment in the presence of *MCPH1* or *Chk1* siRNAs, but not control siRNA. (**e**) Defective ATR-dependent G2–M arrest evident following *MCPH1* siRNA transfection, 24 h after 2.5 J $m^{-2}$ UV. (**f**) *In vitro* expressed MCPH1 and Chk1 interact. Flag-tagged MCPH1 and Myc-tagged Chk1 were expressed and labelled with $^{35}$S-methionine in a rabbit reticulocyte transcription-translation system. MCPH1 was detected in immunoprecipitates using anti-Myc antibodies following co-expression with Chk1. (**g**) Chk1 interacts with a central MCPH1 fragment that lacks BRCT domains. Schematic representation of the constructs used in a GST-pulldown assay. HeLa-expressed Chk1 interacted specifically with non-BRCT containing (NB) fragment even in 3-5 fold excess of GST, GST–B1 and GST–B2B3. GST-fusion protein concentration was estimated by Coommassie blue staining. Full length GST–MCPH1 was insoluble. (**h**) Schematic representation of the role of MCPH1–microcephalin in regulating mitotic entry. Solid lines show steps occuring normally in *MCPH1*-mutant cell lines; dotted lines are defective events (or anticipated defective events). The likely point of MCPH1 function is highlighted. The error bars represent the s.d. of at least three independent experiments.

Immunofluorescence microscopy was used to examine the presence and subcellular distribution of pY15-Cdk1. The limited utility of the pY15-Cdk1 antibody for immunofluorescence precluded precise quantification of pY15-Cdk1 levels. Nevertheless, 33% of control cells with cytoplasmic cyclin B1 staining had detectable colocalized pY15-Cdk1 staining, which was the expected pattern for S–G2 cells (Fig. 4d), whereas pY15-Cdk1 staining was only detectable in 8% of the *MCPH1* -mutant cells with cytoplasmic cyclin B1. This is consistent with the reduced pY15-Cdk1 present in unsynchronized S–G2 *MCPH1*-mutant cells. Strikingly, 100% of PCC cells exhibited diffuse cyclin B1 staining without detectable pY15-Cdk1 (Fig. 4d). In some PCC cells, small pY15-Cdk1 positive foci, possibly representing centrosome-associated pY15-Cdk1, were visible (Fig. 4d). Normal mitotic cells, characterised by nuclear cyclin B1 without detectable pY15-Cdk1, were observed at equal levels in both populations (Fig. 4d).

Immunostaining for lamin B1, a nuclear membrane component normally degraded in late prophase, demonstrated that PCC cells retain an intact nuclear membrane (Fig. 4e). Additionally, PCC cells failed to stain for phospho-S10-histone H3 (a mitotic marker for condensed chromatin), suggesting that they have not progressed into mitosis despite their pY15-Cdk1 status (Fig. 4e). Collectively, these data suggest that PCCs arise as a consequence of inappropriately high Cdk1–cyclin B1 activity in *MCPH1*-mutant cells.

*MCPH1* siRNA causes reduced *Chk1* and *BRCA1* expression in U20S cells, as previously demonstrated[1,2]; it also causes PCC formation (see Supplementary Information, Fig. S3). However, *MCPH1* siRNA in LBLs did not change *Chk1* and/or *BRCA1* expression, yet caused elevated PCC formation, elevated damage-induced nuclear fragmentation, abolished G2–M arrest and reduced pY15-Cdk1, consistent with the findings in *MCPH1*-mutant cell lines (Fig. 5a–c). The lack of impact on *BRCA1* and *Chk1* levels in LBLs may be attributable to less severe depletion or to cell or tissue differences. Taken together, these data demonstrate roles for MCPH1 that are distinct from *Chk1* and *BRCA1* regulation. Furthermore, an interaction between MCPH1 and Chk1 has been identified (Fig. 5f, g), which provides an alternative mechanism for MCPH1 function in Chk1-dependent processes.

Our studies using MCPH syndrome patient cell lines provide a complementary approach to siRNA to examine MCPH1 function and a link to the pathogenesis of primary microcephaly. The normal Chk1 and BRCA1 protein levels in the two *MCPH1*-mutant cell lines used may be a consequence of incomplete loss-of- or separation-of-function due to hypomorphic mutations (see Supplementary Information, Fig. S1). As Chk1 and BRCA1 are essential for cell survival, it is perhaps not surprising that patient mutations do not affect their expression. We have established that incomplete loss-of-function is likely for at least one of the mutations by showing that cells with the truncated MCPH1$^{C74G}$ mutation fail to undergo NMD and have detectable residual protein, possibly due to read-through of an inefficient stop codon created by this mutation[26]. Although residual MCPH1 was not detected in *MCPH1*$^{427insA}$ cells, they potentially express a carboxy-terminal truncated protein.

Our findings highlight two phenotypes conferred by MCPH1 deficiency: the first demonstrates a role for MCPH1 in the ATR-dependent damage response; the second suggests an ATR-independent role. Both *MCPH1*-mutant cell lines show normal ATR-dependent phosphorylation events, demonstrating proficiency in ATR activation. However, like ATR–Seckel cells, they show impaired damage-induced G2–M checkpoint arrest and nuclear fragmentation, as well as supernumerary mitotic centrosomes. They also exhibit inappropriate Cdc25A stabilization, consistent with the lack of Chk1-dependent ubiquitin mediated degradation. Consequently, ATR–Seckel and *MCPH1*-mutant cells fail to diminish chromatin loading of Cdc45 after DNA damage. Cdc25A degradation and G2–M checkpoint arrest are Chk1-dependent events[15,27]. As the *MCPH1*-mutant cell lines show normal Chk1 levels and phosphorylation, and can effect two Chk1-dependent processes (53BP1 foci formation and resumption of DNA synthesis after replication arrest), our findings suggest that MCPH1 has a function downstream of Chk1, but upstream of Cdc25A, in the damage response. Although our studies have focused on ATR-dependent signalling, the impact on Cdc25A could also contribute to defects previously observed in ATM signalling, as Cdc25A impinges on both pathways. However, this cannot be distinguished from the impact on *Chk1* or *BRCA1* transcriptional regulation at the present time.

Cdc25A degradation is impaired in *MCPH1*-mutant and ATR–Seckel syndrome cells, so that the unique PCC phenotype of *MCPH1*-mutant cell lines cannot be attributed solely to aberrant Cdc25A degradation. The distinctions between the phenotype of *MCPH1*-mutant and ATR-deficient cells is as informative as their overlapping characteristics. Importantly, although the level of pY15-Cdk1 is nearly normal in *MCPH1*-mutant cells immediately after release from synchronisation, it rapidly drops with progression through S phase (Fig. 4c) and precedes, but correlates temporally, with PCC formation. Strikingly, PCC cells are pY15-Cdk1 negative and, despite having prematurely condensed chromosomes, have not progressed to the later stages of mitosis (Fig. 4e). Our findings strongly suggest that untimely chromosome condensation occurs in *MCPH1*-mutant cells due to low pY15-Cdk1 levels. Although the failure of ATR–Seckel cells to display PCCs could be attributed to residual ATR activity, we consider this unlikely as, in other assays, *MCPH1*-mutant and ATR–Seckel cells show similar defective phenotypes. Thus, we propose that MCPH1 has additional functions that affect Cdk1-Y15 phosphorylation. Cdc25A undergoes multiple modifications, which are likely to act in a combinatorial manner. Additionally, ATR-independent signalling pathways, including ATM and the p38 MAP kinase stress response pathway, also result in Cdc25A modifications[28]. An appealing model is that MCPH1 serves to co-ordinate Cdc25A modifications, including ATR–Chk1 dependent phosphorylation (Fig. 5h). Another possibility (which is not mutually exclusive) is that MCPH1 regulates proteins other than Cdc25A(such as Cdc25B and C phosphatases or Wee1–Myt1 kinases), which regulate Cdk1 phosphorylation either directly,or indirectly.

Our findings demonstrate a striking correlation between defective ATR-dependent signalling and the occurrence of microcephaly. It is currently unclear which aspect of ATR function may be important — defective G2–M checkpoint arrest and supernumerary mitotic centrosomes are important common phenotypes, and centrosome stability and spindle pole orientation are fundamental for brain development. Significantly, other proteins defective in primary microcephaly (ASPM, CDK5RAP2 and CENPJ) are centrosome-associated[3].

In conclusion, we show that MCPH1 has a function downstream of Chk1 in the ATR-dependent damage-response pathway that affects Cdc25A stability and G2–M checkpoint arrest after DNA damage. This function is in addition to, but distinct from, its role in the transcriptional regulation of *Chk1* and *BRCA1* (ref. 1,2). Additionally, MCPH1 deficiency results in diminished levels of pY15-Cdk1 in late S and G2 phase, which is likely to explain the characteristic PCC phenotype. Taken together, our findings provide strong evidence that MCPH1 has a role in co-ordinating the regulation of Cdc25A and Cdk1–cyclin B1 activity and thus, in regulating mitotic entry. □

## METHODS

**Cell lines and cell culture.** LBLs were cultured in RPMI 1640 with 15% fetal calf serum (FCS). Cells used were GM02188 (control), GM03189D (ATM-defective), DK0064 (ATR–Seckel)[5,6] and are all available from the Coriell Cell Repository (New York, NJ), and NV0001 (*MCPH1*$^{C74G}$)[4] and 563-LBL (*MCPH1*$^{427insA}$)[29]. Primary fibroblast cell lines were cultured in MEM supplemented with 15% FCS. The primary fibroblasts utilised were 1BR3 (control), F02-98 (ATR–Seckel)[5], IN358 (*MCPH1*)[4] and AT5BI (ATM-defective).

**Treatment with DNA-damaging agents.** UV irradiation was carried out using a UV-C source (0.6 J m$^{-2}$s$^{-1}$). APH, hydroxyurea and cytochalasin B were purchased from Sigma-Aldrich (Poole, UK).

**Antibodies and plasmids.** Anti-MCPH1 was directed against full-length GST–MCPH1 and was a generous gift from S.-Y. Lin (The University of Texas MD Anderson Cancer Center, Houston, TX). Anit-KH2AX and anti-pS10 Histone H3 were from Upstate Technology (Buckingham, UK). Anti-pY15-Cdk1, anti-pS317-Chk1 and panti-S15-p53 were from New England Biolabs (Herts, UK). Anti-γ-tubulin and anti-Myc (E10) antibodies were from Sigma-Aldrich . Antibodies against Cdc25A (F-6), Cdc45 (H-300), Cdk1 (A17.1.1), Chk1, Cyclin B1 (GNS1), Grb2 (H-70) and Lamin B1 were from Autogen Bioclear (Whiltshire, UK). Anti-chloro-deoxyUridine and anti-iodo-deoxyUridine were from Abcam (Cambridge, UK) and BD Biosciences (Oxford, UK), respectively and anti-53BP1 (BL181) was from Universal Biologicals (Cambridge, UK). pcDNA3–N-Myc–MCPH1 (C74G) and pcDNA3–C-Myc–MCPH1$^{427insA}$ were derived from pcDNA3–N/C-Myc–MCPH1 using the QuickChange XL site-directed mutagenesis kit (Stratagene, London, UK).

**Immunofluorescence and western blotting.** The immunofluorescence procedure for LBLs cytospun onto poly-L-lysine coated slides was performed as previously described[6,10]. Images were captured using a Zeiss axioplan fluorescent microscope with simple PCI software. For western blotting, 30–50 μg whole cell extracts (WCE; 50 mM Tris–HCl at pH 7.5, 150 mM NaCl, 2 mM EDTA, 2 mM EGTA, 25 mM NaF, 25 mM β-glycerolphosphate, 0.1 mM sodium orthovanadate, 0.2% Triton X-100, 0.3% IGEPAL and protease inhibitor cocktail (Sigma) was resolved by SDS–PAGE, transferred onto PVDF membranes and blocked in 5% BSA–TBS with 0.1% Tween-20. Membranes were probed for pS15-p53 (1:1000), pS317-Chk1 (1:1000), Chk1 (1:300), Cdc25A (1:400), Cdc45 (1:500; 0.2% Tween-20 for all washes), Grb2 (1:500; 0.2% Tween-20 for all washes), pY15-Cdk1 (1:1000) or Cdk1 (1:1000),diluted in 5% BSA–TBS with 0.1% Tween-20, followed by probing with HRP-conjugated secondary antibodies (1:2000; DakoCytomation Ltd, Cambridge, UK).

**Replication-fork stability assay.** The assay was performed as previously described[10]. Briefly, cells were labelled with CldU (50 μM) for 20 mins, pelleted, washed with PBS, resuspended in complete medium with 10 μM APH and incubated for 2 h. These cells were then pelleted and swollen in 75 mM KCl with 50 μM IdUfor 10 mins to allow fork reinitiation and IdU incorporation to occur. After permeabilization, cells were incubated with 2 M HCl for 30 mins to denature the DNA, blocked for 1 h with 10% FCS in PBS and incubated with both primary antibodies overnight at 4 °C. The first label (CldU) was detected with Cy3-conjugated secondary antibody and the second (IdU) with FITC-conjugated antibody (DakoCytomation Ltd, Cambridge, UK).

**G2–M checkpoint arrest and mimosine synchronisation.** The CBPI assay was performed as previously described with some modifications[14]. Cells were pre-incubated for 2 h with 0.1 μM APH, 0.2 mM hydroxyurea or irradiated with 2.5 J $m^{-2}$ UV-C, pelleted, washed and then further incubated for 72 h in the presence of cytochalasin B (5 μg $mL^{-1}$). Cells were processed for immunofluorescence microscopy and cytospun onto poly-L-lysine coated slides.

**Mitotic index.** Cells were irradiated with 2.5 J $m^{-2}$ UV-C, immediately seeded into complete medium with 1.5 μM nocodazole and incubated for 2–24 h before processing for immunofluorescence microscopy with anti-pS10-histone H3 and counterstaining with DAPI.

**Mimosine release.** Cells were incubated overnight in complete medium with 0.2 mM mimosine for synchronisation at G1–early-S-phase. For release, cells were washed and then seeded into complete medium with 1.5 μM nocodazole for 2–10 h before processing for mitotic index. For pY15-Cdk1 western blotting, cells were released into complete medium without nocodazole and collected at 2 and 4 h.

**Nuclear fragmentation.** Cells were treated with 5 mM hydroxyurea in the presence of 1.5 μM nocodazole for 24 h and processed as previously described [6].

**Supernumerary centrosomes.** Cells were incubated for 24 h in the presence of 1.5 μM nocodazole and processed for immunofluorescence microscopy with anti-γ-tubulin antibodies. For each line 50–100 mitotic cells were scored.

**Cdc25A stability assay.** Cells, either untreated or irradiated with 20 J $m^{-2}$ UV-C, were incubated in medium containing 100 μg $ml^{-1}$ cycloheximide. Sampling times of 5–40 min were examined. For full degradation, 20 min was sufficient. Cells were pelleted and resuspended in WCE extraction buffer in the continued presence of cyclohexamide. WCE (50 μg) was fractionated using 8% SDS–PAGE and western blotted with anti-Cdc25A (F-6). Primary fibroblasts were incubated for 4 days to reach confluency before to analysis.

**Chromatin extraction.** The procedure was as previously described with modifications[30]. Unirradiated or irradiated cells ($1.5 \times 10^7$) were washed once in PBS and resuspended in 100 μl E buffer (50 mM HEPES at pH 7.9, 150 mM NaCl, 1.5 mM $MgCl_2$, 0.34 M sucrose, 10% glycerol, 1 mM EDTA, 1 mM DTT, 10 mM NaF, 1 mM $Na_2VO_3$, 10 mM β-glycerolphosphate and protease inhibitor cocktail) with 0.1% Triton X-100. Lysates were incubated on ice for 15 min, repelleted and 50 μg of the supernatant sampled (the soluble fraction). The remaining pellet was washed twice with 200 μl extraction buffer with 0.1% Triton-X-100, resuspended in 50 μl E buffer and dispersed by pipetting. Suspensions were incubated at room temperature for 15 mins in the presence of 200 μg $ml^{-1}$ RNase. Following washing, the chromatin pellets were resuspended in 50 μl of SDS-PAGE loading buffer and sonicated. Finally, 20 μl of the chromatin fraction was separated by 12% SDS–PAGE and western blotted for Cdc45 and Grb2.

**Transfection.** Cells ($3 \times 10^5$ $ml^{-1}$) in 3 ml complete RPMI were transiently transfected with 2 μg pcDNA3–N-Myc–MCPH1, pcDNA3–N-Myc–MCPH1$^{C74G}$ or pcDNA3–C-Myc–MCPH1$^{427insA}$ using Genejuice (Novagen, Madison, WI), according to the manufacturers' instructions, then incubated for 24 h to allow nuclear fragmentation. For complementation of the G2–M checkpoint and supernumerary centrosomes, cells were incubated for 48 h and retransfected for a further 24 h before processing. For the Cdc25A stability assay, transfected cells were incubated for 48 h and retransfected for 48 h before processing.

**RNAi transfection.** The control LBL GM02188 was used for siRNA experiments. Cells were transfected with 10 nM of respective siRNA duplex using SiPort NeoFX transfection reagent according to the manufacturers' instructions (Ambion, Huntington, UK). The oligonucleotides used were: *MCPH1* sense, 5′-CUCUCUGUGUGAAGCACCA-3′; *Chk1* sense, 5′-AAUCGUGAGCGUUUGUUGAAC-3′; and a control oligo directed against *GFP* sense, 5′-AACACUUGUCACUACUUUCTC.

**RT–PCR.** RNA was isolated from LBLs using the RNeasy kit (Qiagen, Crawley, UK) according to manufacturers' instructions. cDNA was generated using random primers and AMV reverse transcriptase (Roche, Welwyn, UK). Duplex PCR was carried out using control primers for Elp4, the constitutively expressed RNA pol II transcription elongation factor: *Elp4F*, 5′-GCGACCGTCGGTGCGGAATGG-3′ and *Elp4R*, 5′-AGAACATAGAGGAACTTGGTAAG-3′ to generate a 700 bp product; and either *MCPH1* primers (A): F, 5′-GCTCGCAAGCACCGCGTAGG-3′ and R, 5′-GGAAAGGAAGTTGGAAGGATCCA-3′ to generate a 810 bp product; or *MCPH1* primers (B): F 5′-GATCCCGCCGTCTGTCATGGC-3′ and R 5′-GAAGAGAGGCGTAAAGCTCG-3′ to generate a 227 bp product. Thirty five cycles of PCR were performed with an annealing temperature of 57 °C.

***In vitro* transcription–translation.** Differentially tagged MCPH1 (pcDNA3.1–N-Flag–MCPH1) and Chk1 (pcDNA3.1–C-Myc–His–Chk1) were co-expressed (2 μg of each plasmid) in the presence of $^{35}$S-methionine using the TNT *in vitro* transcription–translation system (Promega, Southampton, UK) according to the manufacturers' instructions. The reaction products were subjected to immunoprecipitaion using anti-Myc antibodies and resolved on 4–12% NuPAGE (Invitrogen) denaturing gradient gel in MOPS buffer. The gel was fixed, dried and radioactive bands detected by autoradiography.

**GST–MCPH1 fusion.** GST-fusion deletion constructs of MCPH1 were expressed in Rosetta 2 *Escherichia coli*. GST-fusion products were induced by addition of 0.4 mM IPTG at 37 °C for 3 h (GST, B1 and NB constructs) or 0.1 mM IPTG at 25 °C overnight (for B2B3 construct). Following coupling to GS4B beads, the GST-fusion MCPH1 constructs were incubated with 500 μg HeLa WCE and incubated overnight at 4 °C. Following extensive washing (in 50 mM Tris at pH 7.5, 150 mM NaCl, 1% NP40, 0.5% sodium deoxycholate and 0.1% SDS), samples were resolved by 10% SDS–PAGE and probed for Chk1 by western blotting.

*Note: Supplementary Information is available on the Nature Cell Biology website.*

ACKNOWLEDGEMENTS
We are grateful to S.-Y. Lin for the anti-MCPH1 antibody. The P.A.J. laboratory is supported by the Medical Research Council (MRC), the Human Frontiers Science Programme, the Leukaemia Research Fund, the International Agency for Cancer Research and an EU grant (FIGH-CT-200200207). A.P.J. is funded by an MRC Clinical Scientist Fellowship.

AUTHOR CONTRIBUTIONS
The laboratories of P.A.J. and A.P.J. made the major contributions to this work. A.P.J. and members of his laboratory contributed both intellectually and practically to the inception and execution of the work. H.N. provided the *MCPH1*$^{427insA}$ cell line.

COMPETING FINANCIAL INTERESTS
The authors declare that they have no competing financial interests.

Published online at http://www.nature.com/naturecellbiology/
Reprints and permissions information is available online at http://npg.nature.com/reprintsandpermissions/

1. Xu, X., Lee, J. & Stern, D. F. Microcephalin is a DNA damage response protein involved in regulation of *CHK1* and *BRCA1*. *J. Biol. Chem.* **279,** 34091–34094 (2004).
2. Lin, S. Y., Rai, R., Li, K., Xu, Z. X. & Elledge, S. J. BRIT1/MCPH1 is a DNA damage responsive protein that regulates the Brca1–Chk1 pathway, implicating checkpoint dysfunction in microcephaly. *Proc. Natl Acad. Sci. USA* **102,** 15105–15109 (2005).
3. Woods, C. G., Bond, J. & Enard, W. Autosomal recessive primary microcephaly (MCPH): a review of clinical, molecular, and evolutionary findings. *Am. J. Hum. Genet.* **76,** 717–728 (2005).
4. Jackson, A. P. *et al.* Identification of microcephalin, a protein implicated in determining the size of the human brain. *Am. J. Hum. Genet.* **71,** 136–142 (2002).
5. O'Driscoll, M., Ruiz-Perez, V. L., Woods, C. G., Jeggo, P. A. & Goodship, J. A. A splicing mutation affecting expression of ataxia-telangiectasia and Rad3-related protein (ATR) results in Seckel syndrome. *Nature Genet.* **33,** 497–501 (2003).
6. Alderton, G. K. *et al.* Seckel syndrome exhibits cellular features demonstrating defects in the ATR signalling pathway. *Hum. Mol. Genet.* **13,** 3127–3138 (2004).
7. Zou, L. & Elledge, S. J. Sensing DNA damage through ATRIP recognition of RPA-ssDNA complexes. *Science* **300,** 1542–1548 (2003).
8. Shiloh, Y. ATM and ATR: networking cellular responses to DNA damage. *Curr. Opin. Genet. Dev.* **11,** 71–77 (2001).
9. Fernandez-Capetillo, O., Lee, A., Nussenzweig, M. & Nussenzweig, A. H2AX: the histone guardian of the genome. *DNA Repair* **3,** 959–967 (2004).
10. Stiff, T. *et al.* Nbs1 is required for ATR-dependent phosphorylation events. *EMBO J.* **24,** 199–208 (2005).
11. Sengupta, S. *et al.* Functional interaction between BLM helicase and 53BP1 in a Chk1-mediated pathway during S-phase arrest. *J. Cell Biol.* **166,** 801–813 (2004).
12. Zachos, G., Rainey, M. D. & Gillespie, D. A. Chk1-dependent S–M checkpoint delay in vertebrate cells is linked to maintenance of viable replication structures. *Mol. Cell Biol.* **25,** 563–574 (2005).
13. Feijoo, C. *et al.* Activation of mammalian Chk1 during DNA replication arrest: a role for Chk1 in the intra-S phase checkpoint monitoring replication origin firing. *J. Cell Biol.* **154,** 913–923 (2001).
14. Fenech, M. & Morley, A. A. Cytokinesis-block micronucleus method in human lymphocytes: effect of *in vivo* ageing and low dose X-irradiation. *Mutat. Res.* **161,** 193–198 (1986).
15. Mailand, N. *et al.* Rapid destruction of human Cdc25A in response to DNA damage. *Science* **288,** 1425–1429 (2000).
16. Molinari, M., Mercurio, C., Dominguez, J., Goubin, F. & Draetta, G. F. Human Cdc25 A inactivation in response to S phase inhibition and its role in preventing premature mitosis. *EMBO Rep.* **1,** 71–79 (2000).
17. Mailand, N. *et al.* Regulation of G(2)/M events by Cdc25A through phosphorylation-dependent modulation of its stability. *EMBO J.* **21,** 5911–5920 (2002).
18. Chen, M. S., Ryan, C. E. & Piwnica-Worms, H. Chk1 kinase negatively regulates mitotic function of Cdc25A phosphatase through 14–3-3 binding. *Mol. Cell Biol.* **23,** 7488–7497 (2003).
19. Uto, K., Inoue, D., Shimuta, K., Nakajo, N. & Sagata, N. Chk1, but not Chk2, inhibits Cdc25 phosphatases by a novel common mechanism. *EMBO J.* **23,** 3386–3396 (2004).
20. Sorensen, C. S., Syljuasen, R. G., Lukas, J. & Bartek, J. ATR, claspin and the Rad9-Rad1-Hus1 complex regulate Chk1 and Cdc25A in the absence of DNA damage. *Cell Cycle* **3,** 941–945 (2004).
21. Donzelli, M. & Draetta, G. F. Regulating mammalian checkpoints through Cdc25 inactivation. *EMBO Rep.* **4,** 671–677 (2003).
22. Costanzo, V. *et al.* Reconstitution of an ATM-dependent checkpoint that inhibits chromosomal DNA replication following DNA damage. *Mol. Cell* **6,** 649–659 (2000).
23. Bell, S. P. & Dutta, A. DNA replication in eukaryotic cells. *Annu. Rev. Biochem.* **71,** 333–374 (2002).
24. Tercero, J. A., Labib, K. & Diffley, J. F. DNA synthesis at individual replication forks requires the essential initiation factor Cdc45p. *EMBO J.* **19,** 2082–2093 (2000).
25. Gautier, J., Solomon, M. J., Booher, R. N. J. F., Bazan, J. F. & Kirschner, M. W. cdc25 is a specific tyrosine phosphatase that directly activates p34cdc2. *Cell* **67,** 197–211 (1991).
26. Beier, H. & Grimm, M. Misreading of termination codons in eukaryotes by natural nonsense suppressor tRNAs. *Nucleic Acids Res.* **29,** 4767–4782 (2001).
27. Falck, J., Mailand, N., Syljuasen, R. G., Bartek, J. & Lukas, J. The ATM–Chk2–Cdc25A checkpoint pathway guards against radioresistant DNA synthesis. *Nature* **410,** 842–847 (2001).
28. Manke, I. A. *et al.* MAPKAP kinase-2 is a cell cycle checkpoint kinase that regulates the G2/M transition and S phase progression in response to UV irradiation. *Mol. Cell* **17,** 37–48 (2005).
29. Trimborn, M. *et al.* Mutations in microcephalin cause aberrant regulation of chromosome condensation. *Am. J. Hum. Genet.* **75,** 261–266 (2004).
30. Zou, L., Cortez, D. & Elledge, S. J. Regulation of ATR substrate selection by Rad17-dependent loading of Rad9 complexes onto chromatin. *Genes Dev.* **16,** 198–208 (2002).

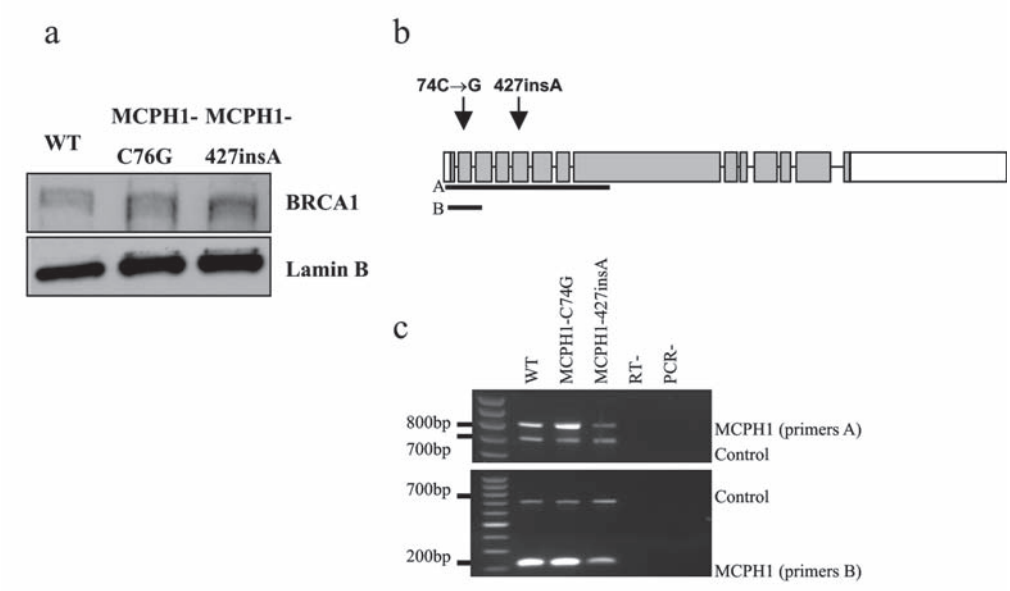


**Figure S1 a**) BRCA1 is expressed at normal levels in MCPH1 cell lines. Since a previous publication using siRNA of MCPH1 had reported that MCPH1 regulated BRCA1 protein levels, we assessed the BRCA1 protein level in MCPH1 cells. Nuclear extracts were separated on 6% polyacrylamide gels and western blotted with the antibodies indicated. No significant decrease in the levels of Chk1 (Fig. 1d) or BRCA1 was observed. **b**) Pictorial representation of the exonic structure of *MCPH1* gene showing sites of the MCPH1 patient mutations and the locations of the primer pairs (A and B) used for the RT-PCR shown in c). Coding exons are shaded. **c**) Characterisation of the impact of the mutational changes in MCPH1 cell lines. Duplex RT-PCR was carried out using MCPH1 specific primers A or B along with control primers towards Elp4 the constitutively expressed RNA pol II transcription elongation factor using MCPH1-C74G and MCPH1-427insA cell lines. Elp4 control primers yield a 700bp product whilst MCPH1-A a 810bp and MCPH1-B a 227bp product. RT- indicates cDNA synthesis reaction without reverse transcriptase, PCR- indicates PCR reaction with addition of template.The transcript present in MCPH1-427insA appears subject to significant but not complete nonsense mediated decay.

***Impact of the mutational changes***: Fig. 1a shows that residual MCPH1-C74G protein is expressed. The mutational change creates a primary UGA stop codon which could be subject to low level readthrough[26]. Additionally, a Kozak consensus transcriptional start site exists 3' of the MCPH1-C74G generated stop codon, which is able to initiate translation in an *in vitro* transcription/translation system (data not shown). However, comparison of the size of the residual protein expressed in MCPH1-C74G cells by Western blotting (Fig. 1a) demonstrated that it was full length and was unlikely to be attributed to a re-initiated product. However, low level expression of a re-initiated protein could also contribute to residual protein function. The MCPH1-427insA transcript is substantially reduced but detectable. Thus, a C-terminal truncated protein could be expressed and could potentially contribute to residual function.

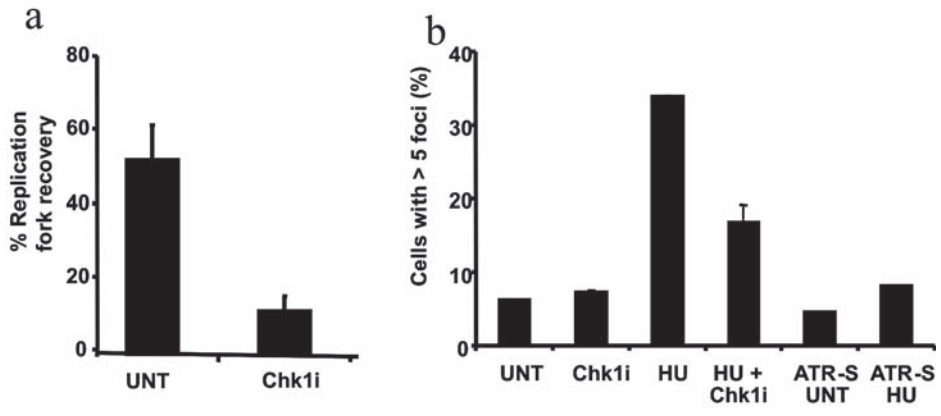


**Figure S2** Pre-treatment of control GM02188 cells with SB-218078 to inhibit Chk1 kinase activity prevents recovery from APH-induced replication fork stalling (**a**) and inhibits HU-induced (5mM 1hr) 53BP1 foci formation (**b**). Cells were pre-treated for 20 mins with 2.5 μM SB-218078 (Chk1i) prior to treatment with APH/HU. SB-218078 was not removed during either experiment. ATR-Seckel cells (ATR-S) are included in b) as a negative control.

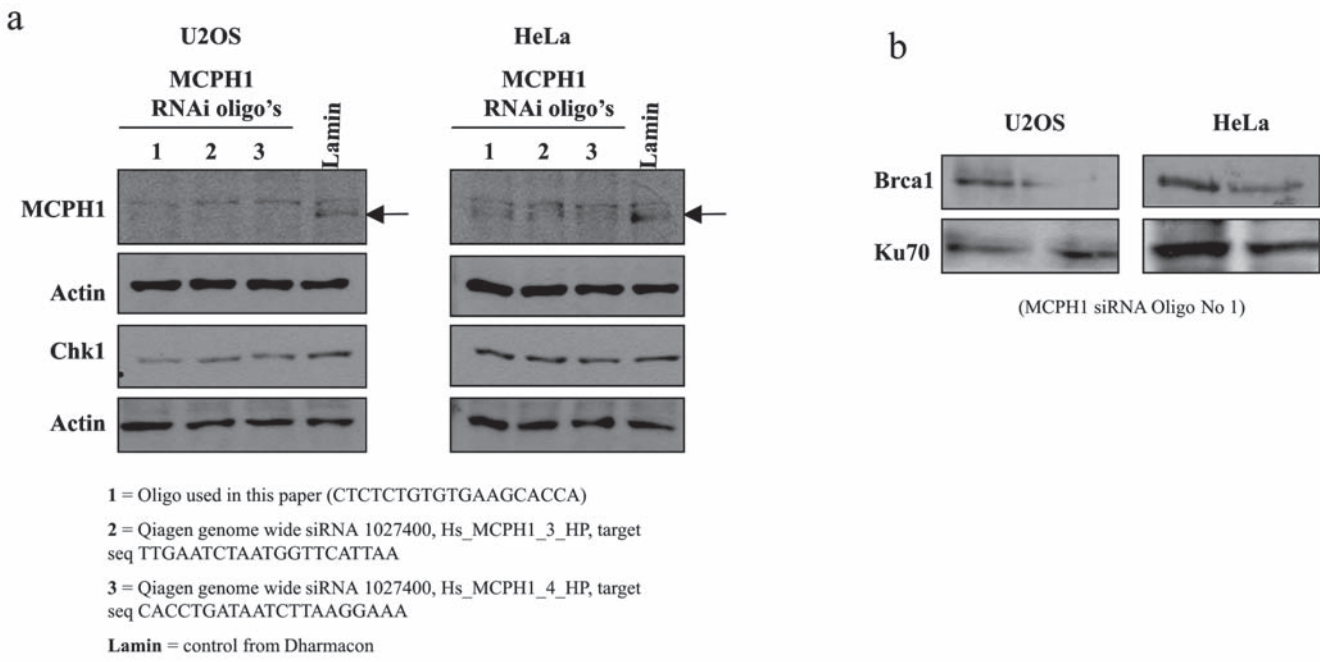


**Figure S3** Three different MCPH1 siRNA oligonucleotides (designated 1-3) were used to evaluate the impact of MCPH1 siRNA. Oligonucleotides to lamin were used as a control. Using U20S cells, all three MCPH1 siRNA oligonucleotides resulted in decreased Chk1 expression (**a**). Oligonucleotide 1 was also used to examine BRCA1 expression, which was also found to be reduced (**b**). None of the oligonucleotides impacted upon Chk1 expression using HeLa cells (**a**), but oligonucleotide 1 also resulted in decreased BRCA1 expression (**b**). siRNA knock down resulted in approximately 20% PCC formation in U2OS cells and approximately 7% in Hela cells. It is possible that the differential impact on Chk1 expression between the cell lines is due to the severity of MCPH1 knock down since some residual MCPH1 expression is clearly visible in the HeLa cells. It is difficult to assess this due to the limited sensitivity of the functional MCPH1 antibodies currently available. An additional contribution to the down regulation of BRCA1 could be impaired cell cycling due to PCC formation following MCPH1 siRNA since BRCA1 expression is specifically high only in S phase cells.

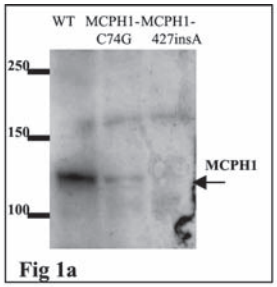


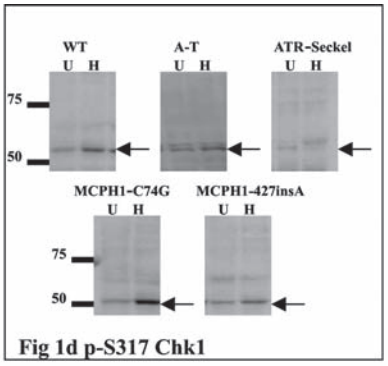


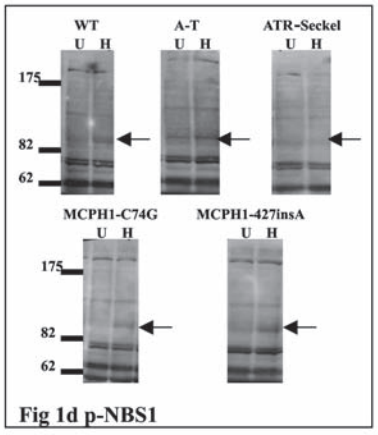


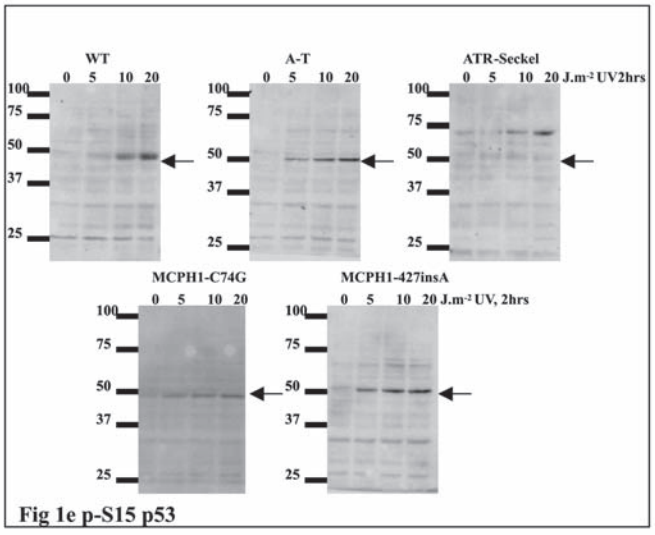


Jeggo Supplementary Figure 4

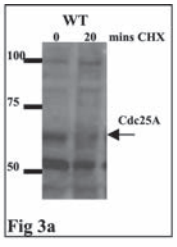


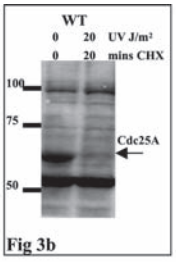


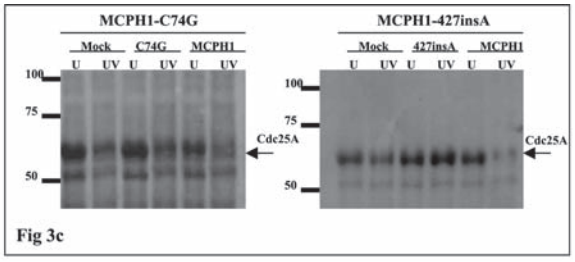


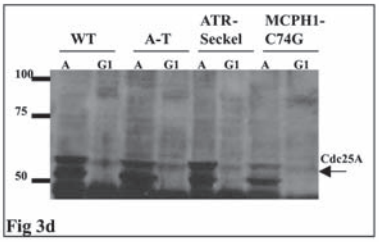


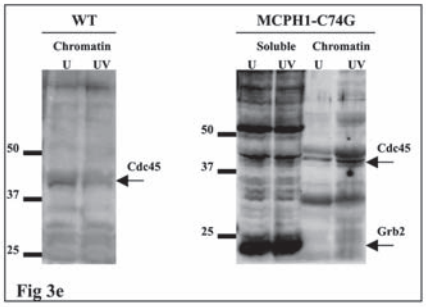


Jeggo Supplementary Figure 4 *cont*

**Figure S4** Expanded blots including molecular weight size markers from selected figures.

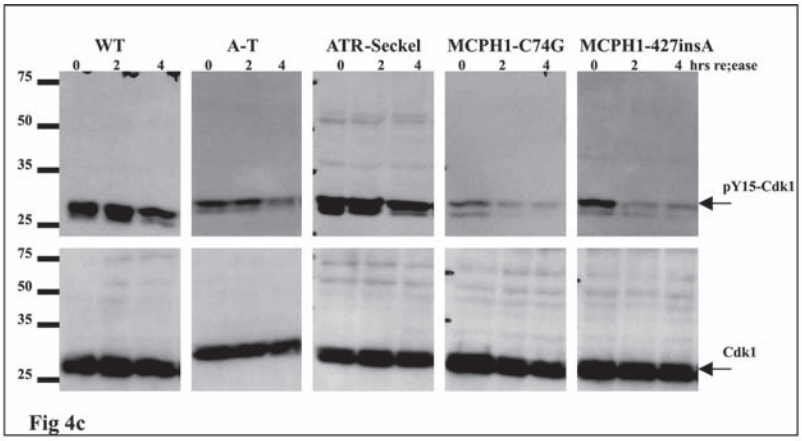


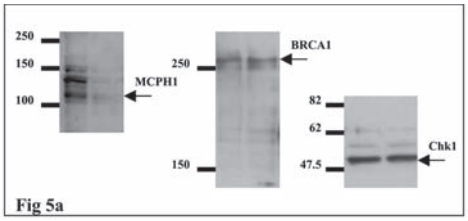


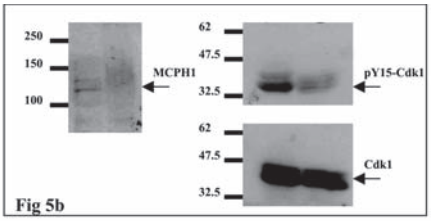


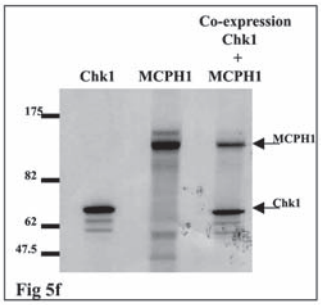


**Figure S4** Expanded blots including molecular weight size markers from selected figures.

**Table S1.**
The PCC phenotype is not present in ATR LBLs

| Cell line | % metaphases (N ) | % interphase (N ) | % PCC cells (N ) |
|---|---|---|---|
| Control | 1.65±0.39 (66) | 98.4 (3941) | 0 (0) |
| ATR-Seckel | 2.28±0.37 (99) | 97.7 (4237) | 0 (0) |
| MCPH1-C74G | 1.68±0.44 (79) | 91.5 (4297) | 6.9±0.72 (322) |

The results represent the average and standard error of 3 independent experiments from asynchronous cell populations. (N) represents the number of cells counted in the 3 experiments.

**Supplementary Material**

***Clinical overlap between MCPH1 primary microcephaly and ATR-Seckel Syndrome:*** Primary microcephaly (OMIM251200) is an autosomal recessive disorder characterised by a marked reduction in brain volume, with a brain size comparable with that of early hominidsS1. MCPH1 primary microcephaly patients also frequently display growth retardation as well as microcephaly (mean head circumference -8 s.d. and height -3 s.d.). Likewise in ATR-Seckel Syndrome (OMIM 210600) patients have greatly reduced head circumferences and heights (-12 and -5 s.d. below the mean respectively) S2. Neither MCPH1 or ATR-Seckel patients have been reported to have immunodeficiency or cancer predisposition, in contrast to other microcephaly syndromes caused by DNA repair proteins (e.g. Nijmegen Breakage Syndrome, and Ligase IV deficiency) S3. In contrast, Ataxia-Telangiectasia, due to mutation of the ATM protein, does not cause a microcephaly syndrome. ATM patients have instead progressive ataxia due to cerebellar degeneration, in association with ocular telangiectasia, chromosome instability and increased cancer susceptibilityS4. Hence, mutations in ATR and MCPH1 cause remarkably similar clinical syndromes, which leads us to hypothesise that the two proteins may act in the same cellular biochemical pathway.

***The MCPH1 Premature chromosome condensation phenotype:*** Approximately 10% of cells in MCPH1 patient cell lines exhibit a premature chromosome condensation (PCC) phenotype, as a result of aberrant regulation of chromosome condensationS5,6. PCCs manifest as prophase-like cells with condensed chromosomes within an intact nuclear envelope. This phenotype is the consequence of early onset of chromosome condensation in the G2-phase of the cell cycle, and delayed decondensation post-mitosisS5,6.


S1. Ponting, C. & Jackson, A.P. Evolution of primary microcephaly genes and the enlargement of primate brains. *Curr Opin Genet Dev* **15**, 241-248 (2005).

S 2. O'Driscoll, M., Ruiz-Perez, V.L., Woods, C.G., Jeggo, P.A. & Goodship, J.A. A splicing mutation affecting expression of ataxia-telangiectasia and Rad3-related protein (ATR) results in Seckel syndrome. *Nat Genet* **33**, 497-501 (2003).

S 3. O'Driscoll, M., Gennery, A.R., Seidel, J., Concannon, P. & Jeggo, P.A. An overview of three new disorders associated with genetic instability: LIG4 syndrome, RS-SCID and ATR-Seckel syndrome. *DNA Repair (Amst)* **3**, 1227-1235 (2004).

S 4. Woods, C.G. DNA repair disorders. *Arch Dis Child* **78**, 178-184 (1998).

S 5. Neitzel, H. *et al.* Premature chromosome condensation in humans associated with microcephaly and mental retardation: a novel autosomal recessive condition. *Am J Hum Genet* **70**, 1015-1022 (2002).

S 6. Trimborn, M. *et al.* Mutations in Microcephalin Cause Aberrant Regulation of Chromosome Condensation. *Am J Hum Genet* **75**, 261-266 (2004).